Supplemental Appendix

Cardiomyocyte proliferation contributes to post-natal heart growth in humans

Mariya Mollova, Kevin Bersell, Stuart Walsh, Jainy Savla, Lala Tanmoy Das, Shin-Young Park, Leslie Silberstein, Cristobal G. dos Remedios, Dionne Graham, Steven Colan, and Bernhard Kühn

Supplemental Information for this manuscript include:

Supplemental Experimental Procedures

Preparation of myocardial samples from healthy human hearts (Sydney, Australia): Obtaining high-quality myocardial samples from newborn babies and young children was a major technical challenge that we needed to overcome in order to accomplish the goals of our study. The muscle research institute at the University of Sydney (Australia) has a tissue bank with healthy human hearts that were procured for transplantation and hence subjected to a strict quality control (short post-mortem interval, standardized preservation procedures). All hearts were removed from the donor and back-flushed with ice-cold cardioplegic solution to remove as much blood as possible (histology showed that there were only occasional blood cells left). They were then double-bagged under sterile conditions and transported by jet plane to the tissue bank in Sydney (**Suppl. Fig. S1A**). The left ventricular (LV) wall was cut from base to apex along the line where the anterior free wall meets the interventricular septum (**Suppl. Fig. S1B**). This process was repeated for the posterior LV wall. The subauricular and subatrial papillary muscles were removed and the remaining tissue was cut into approximately 1 cm-wide strips of the LV free wall and then divided into smaller (1 g) pieces that were immediately flash frozen and then stored in liquid nitrogen (**Suppl. Fig. S1C, D**). The samples were sent to Children's Hospital Boston, embedded in random orientation (OCT, Triangle Biomedical Sciences) and stored in a –80 º C freezer. We prepared cryosections (14 and 30 μm) with a cryostat (CM3050S, Leica) and adhered three consecutive sections per slide to positively charged glass slides (Colorfrost, Fisher).

Preparation of myocardial samples from human cadaveric hearts (Baltimore, USA): We selected hearts from the NICHD Brain and Tissue Bank for Developmental Disorders

(University of Maryland, Baltimore, MD). The samples had post-mortem times of less than 24 hr, were flash-frozen, and stored in liquid nitrogen. These myocardial samples were then processed in the same way as the samples from donor hearts (**Suppl. Fig. S2, Suppl. Tab. S1**).

Analysis on myocardial sections: We selected slides for staining in a random-systematic fashion[1]; that is we selected the first slide to be between number 1 and 10 with a random number generator and then selected every fifteenth slide. We prepared 210 consecutive sections for every heart, three sections per slide, which we coded in such a way that the age of the sample was not identifiable by the analyzing researchers. To quantify myocardial fibrosis, we stained 15 cryosections per heart with acid fuchsin orange-G (AFOG) and took 15 random images on each section (Zeiss AxioPlan2, ×20 lens). We quantified scar size from these images using Metamorph software *via* digital color thresholding (Metamorph, Molecular Devices). Cardiomyocytes and their nuclei were identified using two different structural markers (troponin I and caveolin 3, **Suppl. Fig. S3**); 15 random images per slide were taken with Olympus IX-81 epifluorescence microscope, x60 lens) and number of nuclei was quantified using the optical dissector method[1].

Six blinded observers, unaware of the samples' corresponding ages, performed all quantifications.

Validation of the method for identifying cardiomyocyte nuclei using immunofluorescent microscopy: Sections from human neonatal and adult hearts were stained with cardiomyocyte-specific antibodies against troponin I and caveolin 3. Nuclei were stained with DAPI. Cardiomyocytes were identified in counting frames (131 x 131 μm) using both structural markers and counted with the optical dissector method. Counts were compared by linear

regression analysis. There was a significant correlation between both methods for cardiomyocyte identification r^2=0.8. Bland Altman analysis demonstrated substantial agreement between the two methods for cardiomyocyte quantification (**Suppl. Fig. S3**).

Analysis of isolated cardiomyocytes using laser-scanning cytometry (LSC): Using an automatized method, such as an LSC platform, enabled us to perform analysis on large populations of heart muscle cells in an unbiased, observer-independent fashion. The isolated cardiomyocytes were blocked in blocking medium (5% goat serum, 0.05% Tween-20 in Ca^{2+}-free, Mg^{2+}-free D-PBS) for 10 min before immunofluorescent staining with antibodies against phosphorylated histone H3 (Ser10, rabbit, 1:500, Upstate) and sarcomeric α-actinin (mouse, 1:500, Sigma). The primary antibodies were visualized with anti-mouse Alexa 564 and anti-rabbit Alexa 488 conjugated secondary antibodies (Invitrogen). Nuclei were then labelled with 50 nM DAPI (Invitrogen) and the cardiomyocyte suspensions were spread on glass slides. Coverslips (no. 1.5, VWR) were placed on cardiomyocytes in a water suspension. For LSC analyses, the iCys® Research Imaging Cytometer (CompuCyte Corp.) with four excitation lasers (405, 488, 561, and 633 nm), four emission filters (430-470, 500-545, 565-595, 650 nm long pass), and four photomultiplier tubes (PMT), each detecting a specific wavelength range, was used. PMT signals were converted into 14-bit pixel values that were assembled into high-resolution images at an X step size of 1 μm per pixel. The quantitative imaging cytometry control software (CompuCyte Corp.) generated a sequence of high-magnification (20x objective) 'field' immunofluorescence images which were subjected to automated analysis of contour-based cellular events, nuclear events, and their fluorescence levels. For each fluorescent marker, images were built pixel by pixel from the quantitative PMT measurements of laser-spot-excited fluorescence[2]. Individual cellular events were defined by threshold contouring of α-actinin stained cytoplasm. Individual nuclear events were defined by threshold contouring of DAPI

stained nuclei. The numbers of nuclei in each cell were defined by nuclear events within the integration contour of cellular events. The integration contour was set as 7 pixels out from the threshold contour of cellular events (pixel size was 1 μm x 0.491 μm). The total fluorescence intensity of H3P was measured in the green channel within the integration contour of cellular events. Ploidy quantifications were performed on the basis of DAPI nuclear staining (blue), which allows analysis of both DNA content (integral value) and chromatin concentration (maximum pixel intensity). We validated the LSC-based method of quantifying the amount of DNA in each cardiomyocyte nucleus using human umbilical vein endothelial cells, which are known to be diploid (2N), as control (**Suppl. Fig. S4**). At least 15,000 cardiomyocytes per heart were analyzed per sample.

Validation of ploidy measurement using human umbilical vein endothelial cells as diploid control: Laser-scanning cytometry (LSC), FACS, measures the relative amount of fluorescence. To calibrate the DNA quantification, obtaineed with LSC, we used synchronized human umbilical vein endothelial cells (HUVEC, Lonza, cc-251). G1/S phase cell cycle arrest was induced with double thymidine block. HUVEC were cultured in EGM®-2 Endothelial Cell Growth Medium-2 (Lonza CC-3156) media to confluence in serum rich-media supplemented with FBS, hydrocortisone, hFGF-B, VEGF, R3-IGF-1, ascorbic acid, hEGF, GA-1000, and heparin (10% FCS, 1% Pen-Strep, 1% glutamine) and 2 mM thymidine (Sigma T1895-1G) for 16 hours. Cells were washed 3 x with PBS and fresh EndoGRO added to release cells for 9 hours. After releasing, cells were cultured in serum-rich media with 2 mM thymidine for an additional 17 hours. Thereafter, cells were washed in PBS, trypsinized and fixed in 3.7% paraformaldehyde. HUVEC cells were washes 3x PBS and spun down 3000 rpm. Cells were stained with Cell Mask™ (Invitrogen C10045) and DAPI. Cells washed 2 x PBS and dehydrated onto polylysine-charged slides and cover-slipped. Ploidy was assessed by LSC (**Suppl. Fig. S4j**).

Microscopy and immunofluorescence: To identify desmosomes, we used a rabbit anti-pan-cadherin (Sigma, Cat# C3678, 1:500) and to identify cardiomyocyte cell membranes we used a mouse caveolin 3 antibody (Cat#610421, BD Transduction Labs, 1:100). To identify cardiomyocyte sarcomeres, we used primary antibodies against tropomyosin (Developmental Studies Hybridoma Bank, 1:100) and sarcomeric α-actinin (Sigma, 1:500), and coupled them with Alexa-fluorophore-conjugated secondary antibodies (Invitrogen) (**Suppl. Tab. S4**). Nuclei were visualized with 4', 6'-diamidino-phenylindole (DAPI, Invitrogen, 1:5000). The γ value for image acquisition was set at one. Lookup stable settings were linear. Karyokinesis was visualized with an antibody against phosphorylated histone H3 (Upstate, 1:500) and a monoclonal antibody against the centralspindlin component MKLP-1 (Abcam, 1:100) was used to detect cytokinesis. Images were obtained using a spinning disk confocal microscope (DSU, Olympus) and a laser- scanning confocal microscope (FV1000, Olympus) (**Suppl. Tab. S2**). Three-dimensional reconstructions of the MKLP-1 positive events are shown as separate movies (**Supplemental Movies S1-S4**).

Quantification of mean cardiomyocyte volume: To determine the cellular volumes of isolated cardiomyocytes, we visualized the cytoplasm with CellMask (5 μg/mL, 5 min incubation at room temperature, Invitrogen) and spread the cardiomyocytes on slides. To select cardiomyocytes for volume analysis, we scanned the stained slide with a × 60- water lens and selected one random cardiomyocyte from every 4th field of view. We acquired confocal stacks with a step size of 1.2 μm (Olympus FV 1000, **Suppl. Fig. S5a**). We used digital thresholding to determine the area of each optical section (Image J, **Suppl. Fig. S5b**). Using the area of each optical section and the 1.2 μm between them, we computed the cellular volume. The average cardiomyocyte volume for each heart was determined by calculating the mean ± SEM of 60-100 isolated cardiomyocytes from each heart.

Comparison of design-based and model-based stereological methods for quantification of cardiomyocyte cell volume: In order to validate our cardiomyocyte volume analysis, we applied two different methods. We first used digital color thresholding in 3D- reconstructions of confocal Z-stack images of isolated heart muscle cells and then compared this design-based method to a model that assumed a cylindrical shape for the cardiomyocytes[2]. We performed a Bland-Altman test to determine the agreement between the two methods and a linear regression analysis to see whether the difference between the two methods changed with changing size of the cardiomyocytes. A total of 129 young and 127 adult cardiomyocytes were investigated.

The results show a significant agreement between our designed-based method and model-based methods that have been previously reported in the literature[2]. *P*- values in both the young and the adult hearts were < 0.05, indicating a significant agreement of both methods, irrespective of age **(Suppl. Fig. S5c,d)**.

Quantification of tissue shrinkage: Fixation and staining procedures inevitably lead to tissue shrinkage- a factor that should be considered when quantifying events on three- dimensional tissue sections in order to avoid introducing systematic bias to the volume analyses.

To determine tissue shrinkage in x and y direction, we measured the area per point on phase images of our sections, overlaid with a grid of known dimensions (grid point method)[3] (**Suppl. Fig. S6**). The area per point *a* (point) is the product of the distances between points in the x- and y –directions. The number of points *P* hitting the profile of a section was counted and the total area of a section *A* was estimated according to the formula: $A=\sum P$ x a (p). Measurements before and after fixation and staining were made and the percentage of tissue area shrinkage was calculated.

For tissue shrinkage estimation in the z-dimension, using confocal microscopy, a Z-stack was taken across the whole depth of a section prior to and after fixation and staining procedures. The

thickness of each section was determined at 10 random spots for every section by using the full width at half maximum (FWHM) intensity after plotting the projection of the corresponding grey value profile in Image J. (**Suppl. Fig. S6**). The combination of xy- and z-dimensional measurements resulted in a correction factor of 21 ± 5.8% (mean ± SEM) for tissue shrinkage upon fixation and staining.

Quantification of the number of cardiomyocytes per heart: Cardiomyocyte nuclei were counted using the optical dissector method[1] on 14 μm cryosections that were stained with α-actinin or tropomyosin to identify cardiomyocytes and with DAPI to identify nuclei. We used a spinning disc confocal microscope (Olympus DSU) with a 60x water lens to capture two confocal slices, which were 5 μm apart in the z-axis. One image was used as the counting plane and the other as lookup plane, as described[1,4]. In the counting plane, we counted only those nuclei that were completely surrounded by cardiomyocyte cytoplasm and that were absent from the lookup plane. For this analysis, the first slide from each sample was selected to be between number 1 and 10 using a random number generator. The next slide was selected by successively adding 10 to the random number. Three random sample volumes were counted in this way per section, amounting to 15 sample volumes per heart. The number of cardiomyocyte nuclei per LV was calculated by multiplying the number of cardiomyocyte nuclei per cm^3 (cardiomyocyte nuclear density) with the LV reference volume[5].

Determination of LV reference volume: Weight is the recommended stereological parameter to determine the reference myocardial volume of the heart[1,4]. Exact donor heart weights were available for 7 of the samples studied. To assess LV myocardial growth[5] for the rest of the samples, echocardiographic data from 576 healthy humans in the age range 0-20 years were

obtained from an IRB-approved study at Children's Hospital Boston. The relationship of BSA to myocardial mass was determined using the LMS method as described in [6]. The LV mass for each donor heart was calculated as the mean predicted left ventricular mass for body surface area based on the relationship determined in this normal population. Quantification of stereological parameters of the heart using the calculated heart weights matched very closely with estimations based on actual heart weights for those hearts where this information was available (**Supplemental Figure S8**).

Supplemental Figure and Legend S1

a

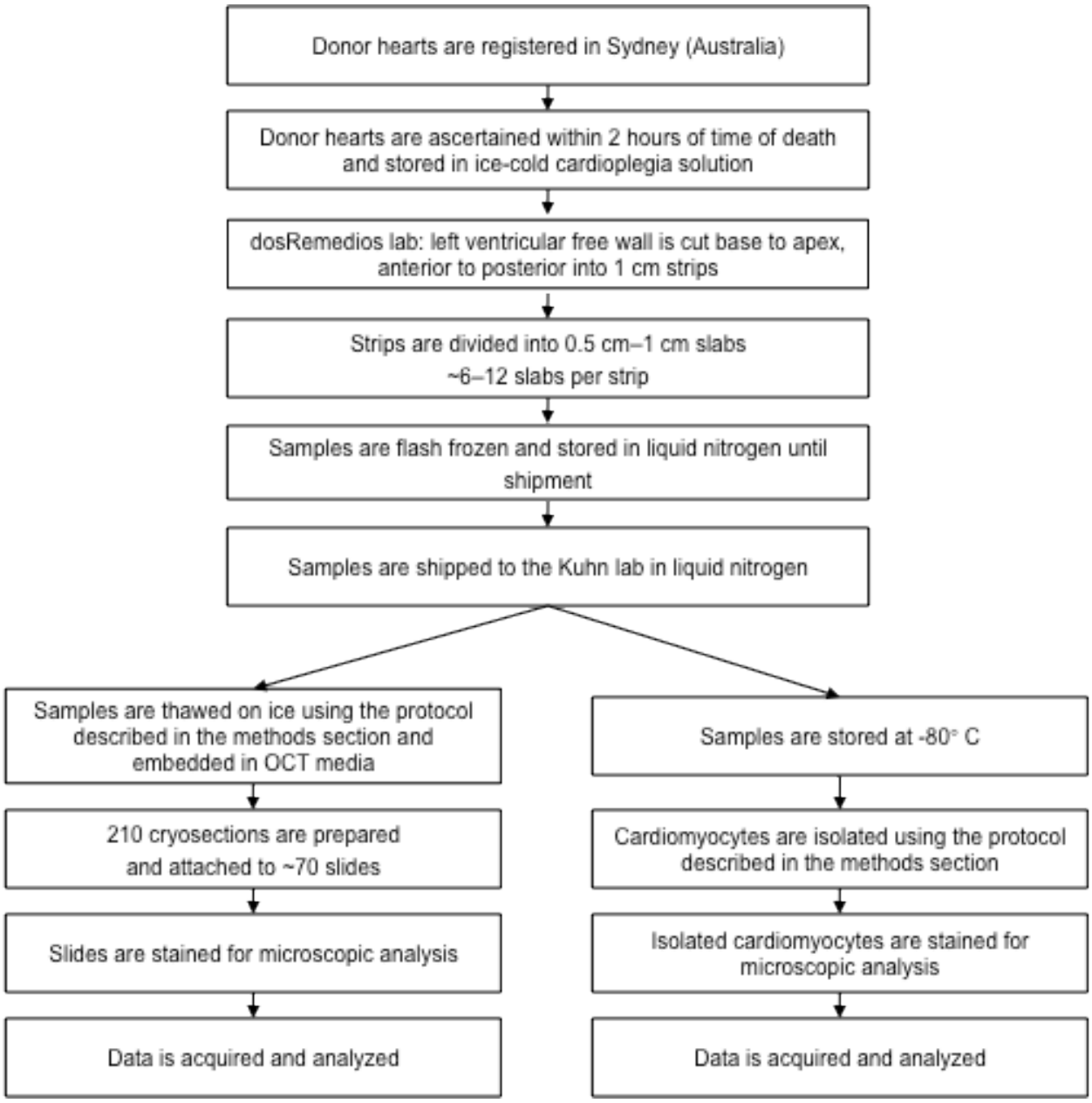

Supplemental Figure S1. Workflow from donor hearts to sample analysis.

(**a**) Flow diagram highlights the key steps of tissue collection, sample acquisition, storage, transportation and analysis.

Supplemental Figure and Legend S1, continued.

b

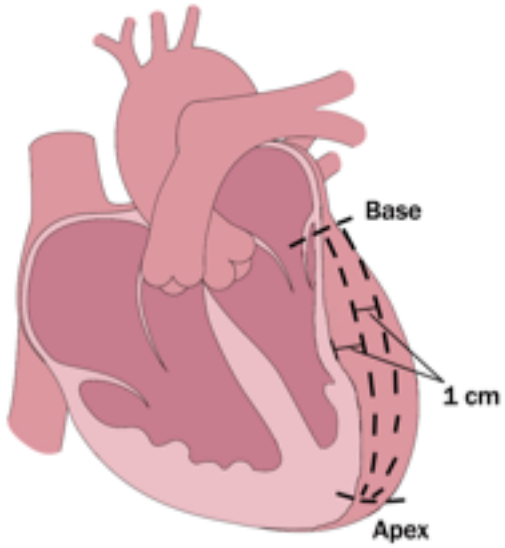

c

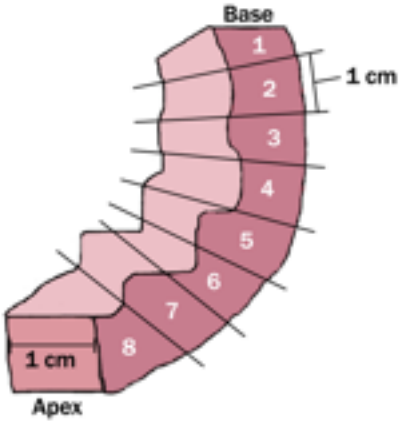

d

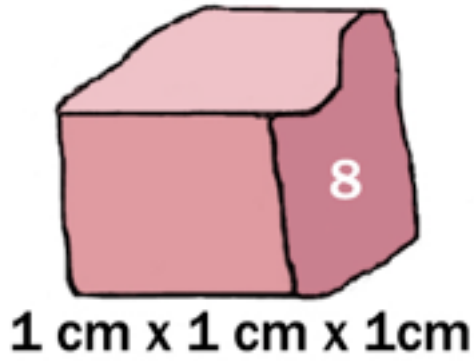

Supplemental Figure S1, continued. Workflow from donor hearts to sample analysis.

(**b**) After cutting along the anterior margin between the interventricular septum and the left ventricular free wall from the base to the apex, parallel strips of myocardium were cut in 1 cm distance, moving from anterior to posterior. (**c**) The 1 cm strips were then divided into 1 cm x 1 cm cubes and flash-frozen in liquid nitrogen. The time from removing the heart from cardioplegia solution to freezing of the last sample was less than 45 min. (**d**) Diagram of one myocardial sample used for analysis.

Supplemental Figure and Legend S2

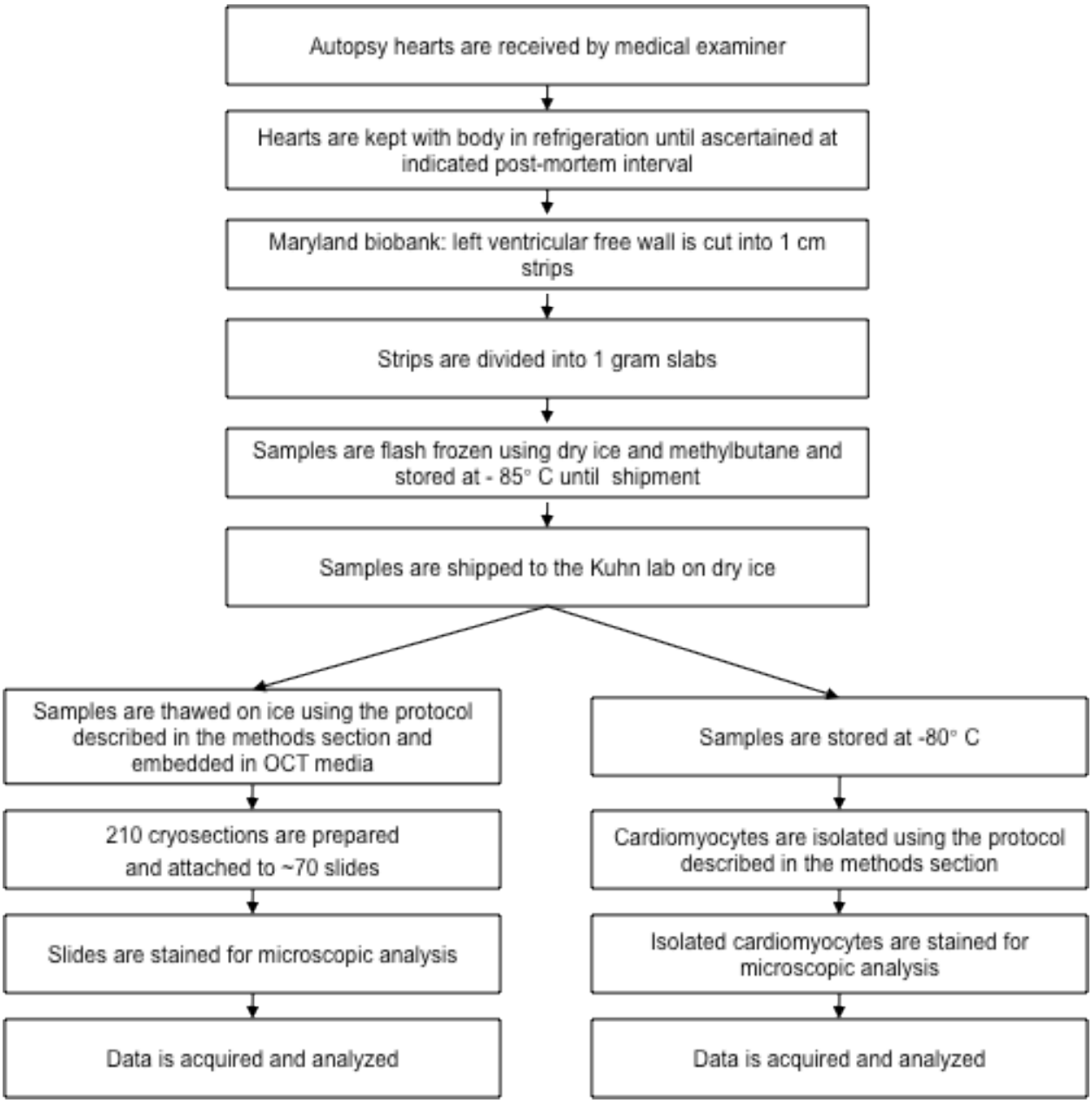

Supplemental Figure S2. Workflow from sample ascertainment to data analysis for cadaveric hearts.

The hearts from the Maryland Hybridoma tissue bank were obtained from human cadavers within 4-23 hr of death. The hearts were kept refrigerated with the body until the medical examiner provided the body to the University of Maryland. They were cut into smaller samples, and flash-frozen with dry ice and methylbutane.

Supplemental Figure and Legend S3

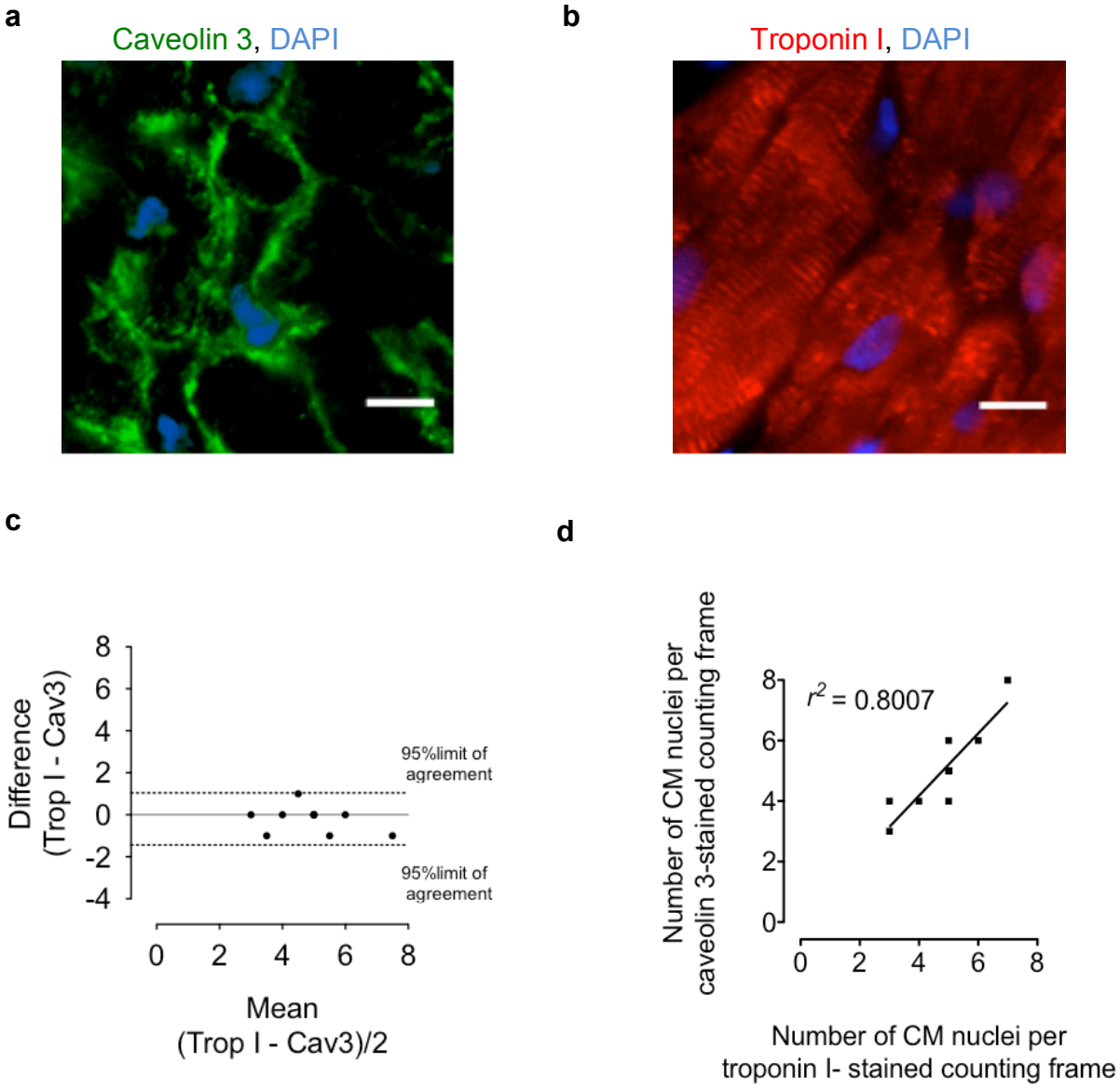

Supplemental Figure S3. Validation of the immunofluorescent identification of cardiomyocytes for the optical dissector method.

Sections from human neonatal and adult hearts were stained with antibodies against troponin I and caveolin 3. Nuclei were stained with DAPI. Cardiomyocytes were identified in counting frames (131 x 131µm) and counts were analyzed by linear regression. (**a**) Caveolin 3 staining. (**b**) Troponin I staining, Scale bar 10 µm. (**c**) Bland Altman analysis demonstrates agreement between the two methods for cardiomyocyte quantification. (**d**) Linear regression demonstrates a high correlation between the number of cardiomyocytes identified by caveolin 3 and troponin I antibody.

Supplemental Figure and Legend S3, continued

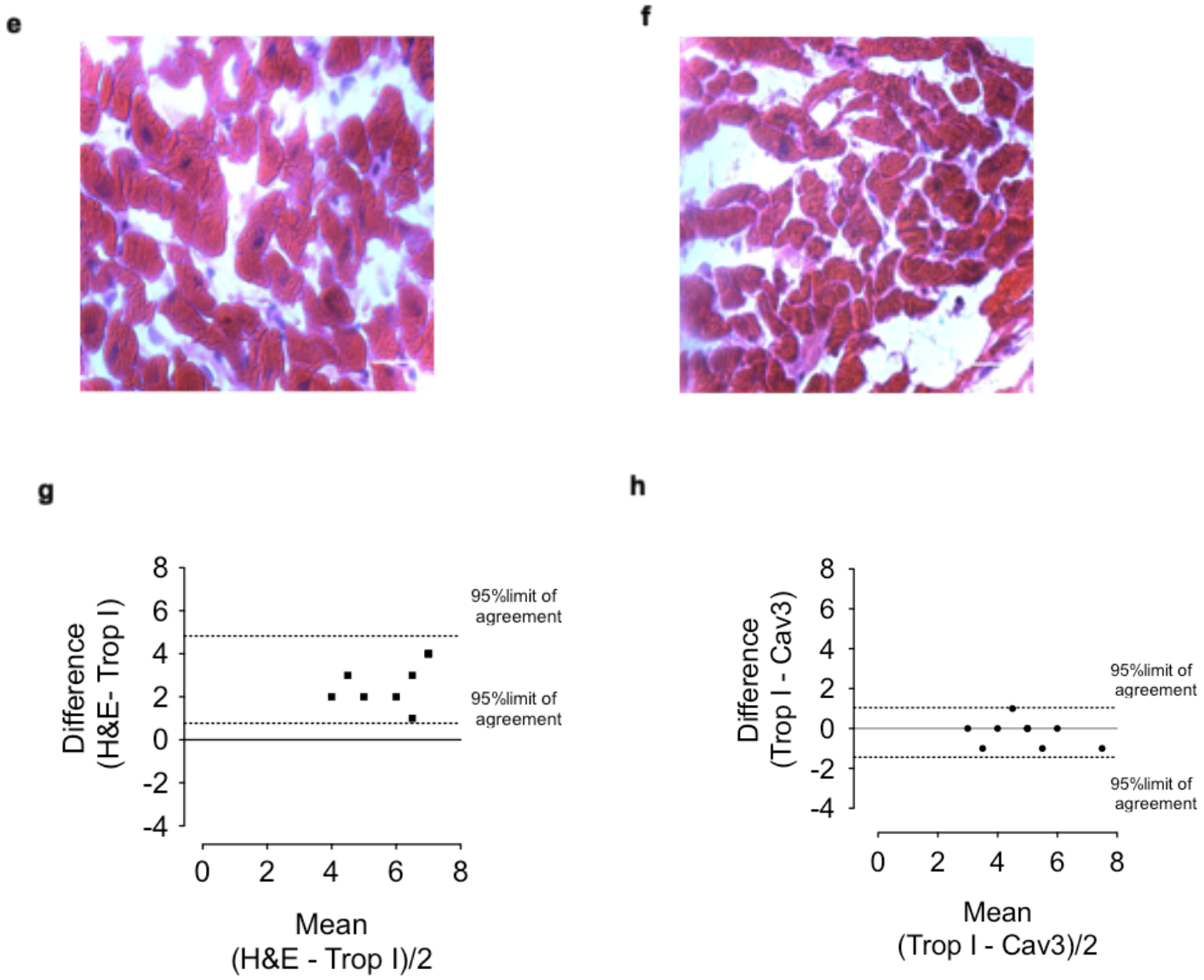

Supplemental Figure S3, continued. Validation of the immunofluorescent identification of cardiomyocytes for the optical dissector method.

Sections from human neonatal (**e**) and adult (**f**) hearts were stained with haematoxylin- eosin (H&E). Mean number of cardiomyocytes was determined per counting frame (131 x 131 µm) and compared to the quantification from the optical dissector method. Scale bar 25 µm. (**g**) Bland Altman analysis demonstrates slight overestimation of cardiomyocyte counts using the haematoxylin-eosin staining versus the optical dissector with antibody against troponin I. (**h**) Bland Altman analysis shows a good agreement between troponin I and caveolin 3 in the quantification of cardiomyocytes with the optical dissector method.

Supplemental Figure and Legend S4

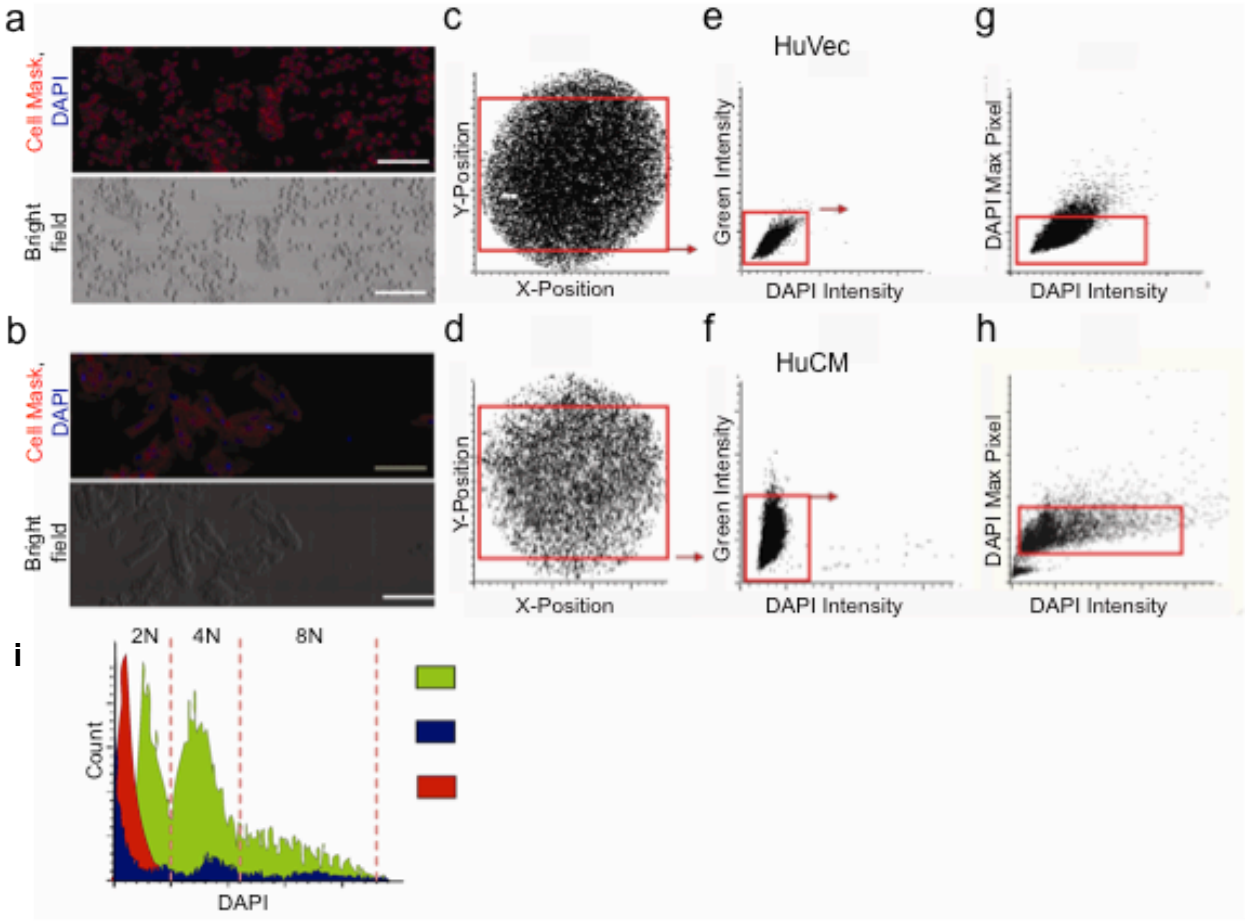

Supplemental Figure S4. Method of ploidy quantification in isolated human cardiomyocytes using laser-scanning cytometry (LSC).

(**a**-**e**) Calibration of the method. Human umbilical cord endothelial cells (huVec), being uniformely mononucleated with diploid nuclei (2N), were used as control to determine DNA content by LSC. Isolated huVec (**a**,**c**,**e**,**g**) and cardiomyocytes (HuCM, **b**,**d**,**f**,**h**) were stained with Cellmask™ membrane dye and DAPI and spread on slides. (**a**, **b**) Representative LSC photomicrographs of immunofluorescence (top panel) and bright bright field (bottom panel). Scale bars 100 µm. huVec (**c**) and cardiomyocyte (**d**) preparations were gated through X and Y positions and autofluorescent artefacts were excluded (**e**,**f**). Individual nuclear events were defined by threshold contouring of DAPI stained nuclei. The numbers of nuclei in each cell are defined by nuclear events within the integration contour of cellular events. The integration contour is set as 7 pixels from the threshold contour of cellular events (pixel size is 1µm x 0.491µm)(**g**, **h**). DNA content histogram (**i**) established by DAPI integrated fluorescence signal in cycling huVec cells (blue plot) and human cardiomyocytes (green plot). HuVec cells were synchronized in G_0/G_1 of the cell cycle with a double thymidine block to establish diploid DNA content threshold settings (red plot).

Supplemental Figure and Legend S4, continued

j

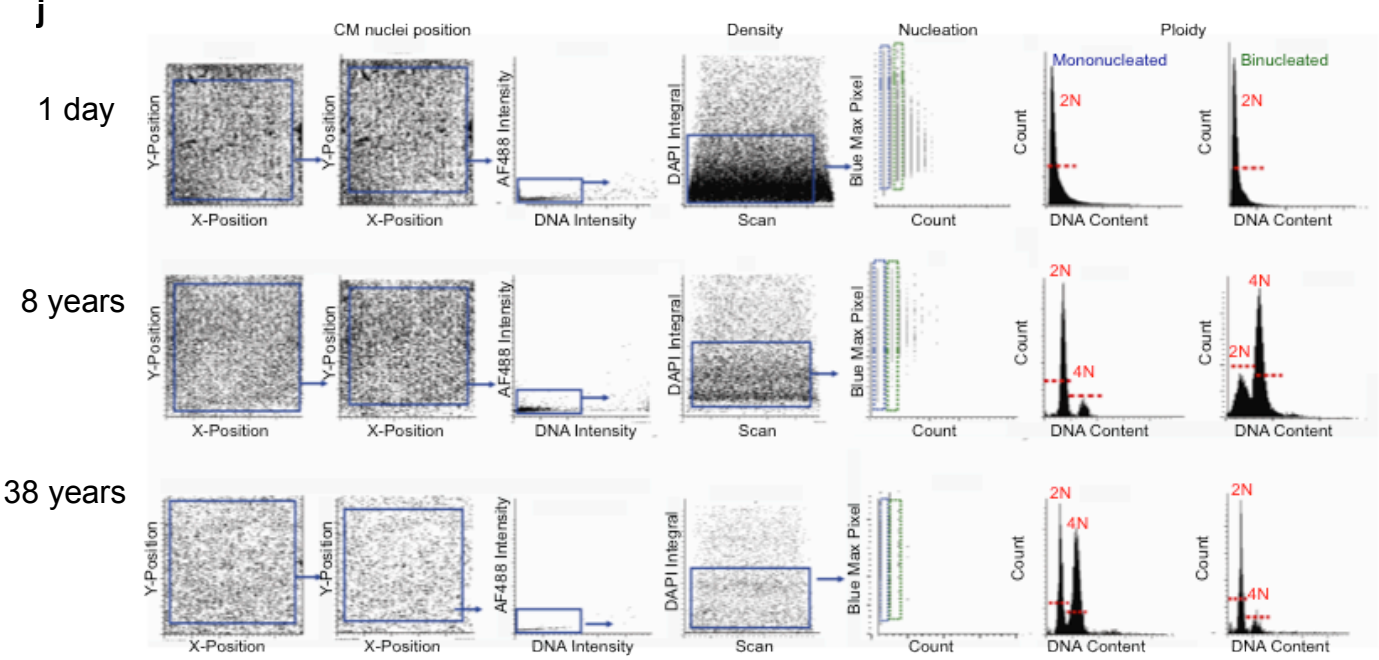

Supplemental Figure S4, continued. Method of ploidy quantification in isolated human cardiomyocytes using laser scanning cytometry (LSC).

(**j**) Representative examples of ploidy quantification in spreads of isolated human cardiomyocytes for a 1-day-old newborn, an 8-year-old child, and a 38-year-old adult are shown. Isolated cardiomyocytes were stained with antibodies against α-actinin and DAPI, immobilized on slides, and scanned by LSC (x20 objective lens). For each fluorescent marker, images are built pixel by pixel from the quantitative PMT measurements of laser-spot-excited fluorescence signals (Grierson et al., 2005). Individual cellular events are defined by threshold contouring of α-actinin stained cytoplasm. Individual nuclear events are defined by threshold contouring of DAPI stained nuclei. The numbers of nuclei in each cell are defined by nuclear events within the integration contour of cellular events. Using the quantitative imaging cytometry control software (iCys, Compucyte) high-magnification immunofluorescence images were subjected to automated analysis of contour-based cellular events, nuclear events, and their fluorescence levels. Individual cardiomyocytes were analyzed by their X and Y-position on the slides determined by α-actinin fluorescence and nuclei by DAPI fluorescence, respectively (1st and 2nd column). Autofluorescence threshold signals and signal densities removed artifacts, cell aggregates, and other non-specific events (3rd and 4th columns). Mono- and binucleated cardiomyocytes were identified by density of DAPI pixel signals per single α-actinin fluorescent signal (5th panel). The ploidy levels of mono- (6th panel) and binucleated (7th panel) cardiomyocyte populations were assessed separately. In a 1-day-old newborn (top row), the ploidy levels of both mono- and binucleated cardiomyocytes were 2n: >99%, i.e. most cadiomyocytes were diploid. In an 8-year-old child (middle row), the ploidy levels of mononucleated cardiomyocytes were 2n: 82%, 4n: 16%, and >4n: 2% and in binucleated cardiomyocytes 2n: 28%, 4n: 69%, and >4N: 3%. In the 38-year-old adult (bottom row), the ploidy levels of mononucleated human cardiomyocytes were: 2n: 36%, 4n: 58% and >4n: 6% and in binucleated cardiomyocytes 2n: 73%, 4n: 22% and >4n: 5%.

Supplemental Figure and Legend S5

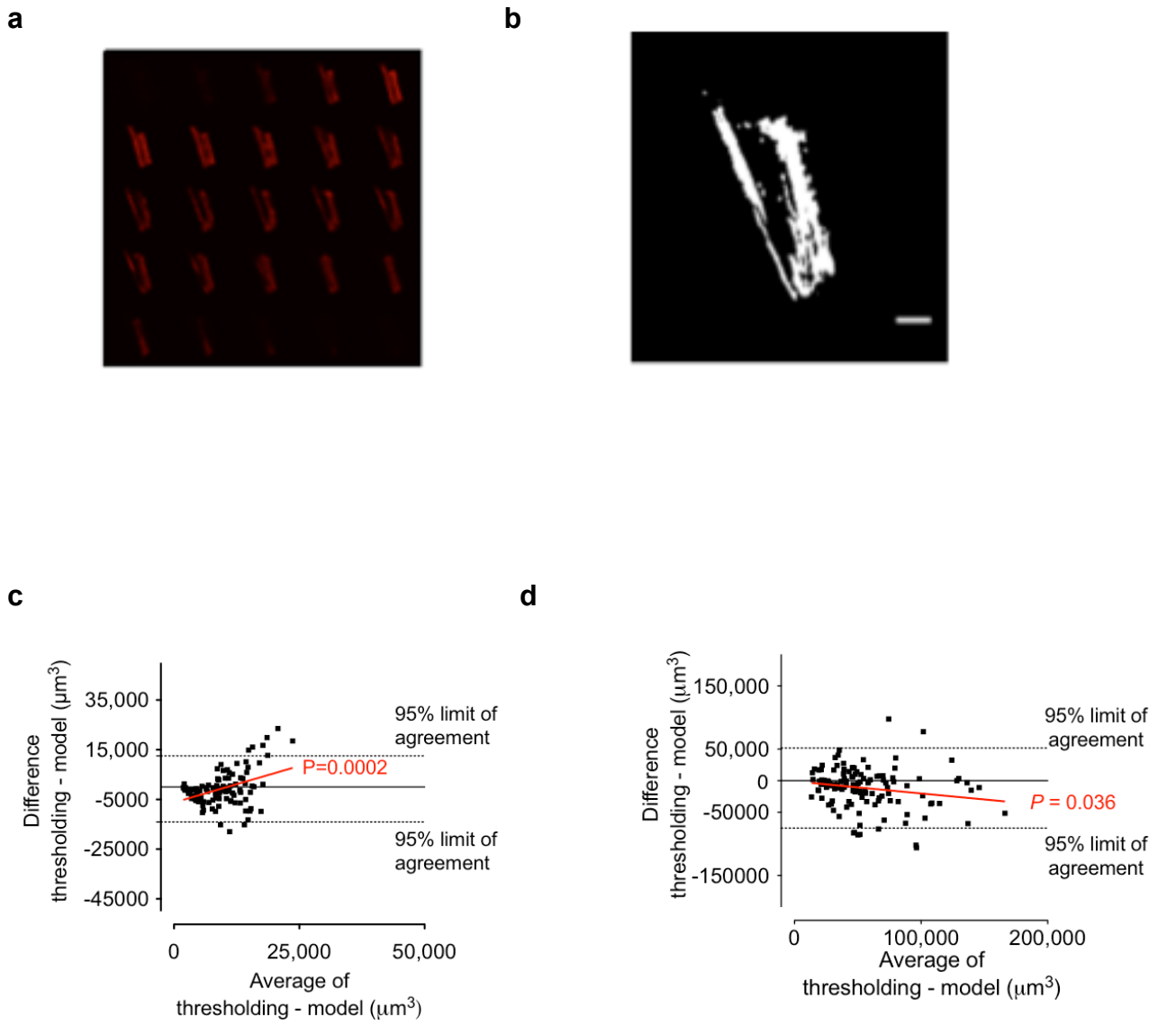

Supplemental Figure S5. Method for quantification of mean cellular volume.

For volume determination, cardiomyocytes were isolated, stained with CellMask Orange and imaged with confocal microscopy. (**a**) Photomicrographs of all optical sections of one representative cardiomyocyte. (**b**) A single optical section used for digital color thresholding. (**c**) Comparison of agreement between design-and model-based method using Bland-Altman analysis in three neonatal hearts (P = 0.0002). (**d**) Comparison of agreement between both methods in three adult hearts (P= 0.036).

Supplemental Figure and Legend S6

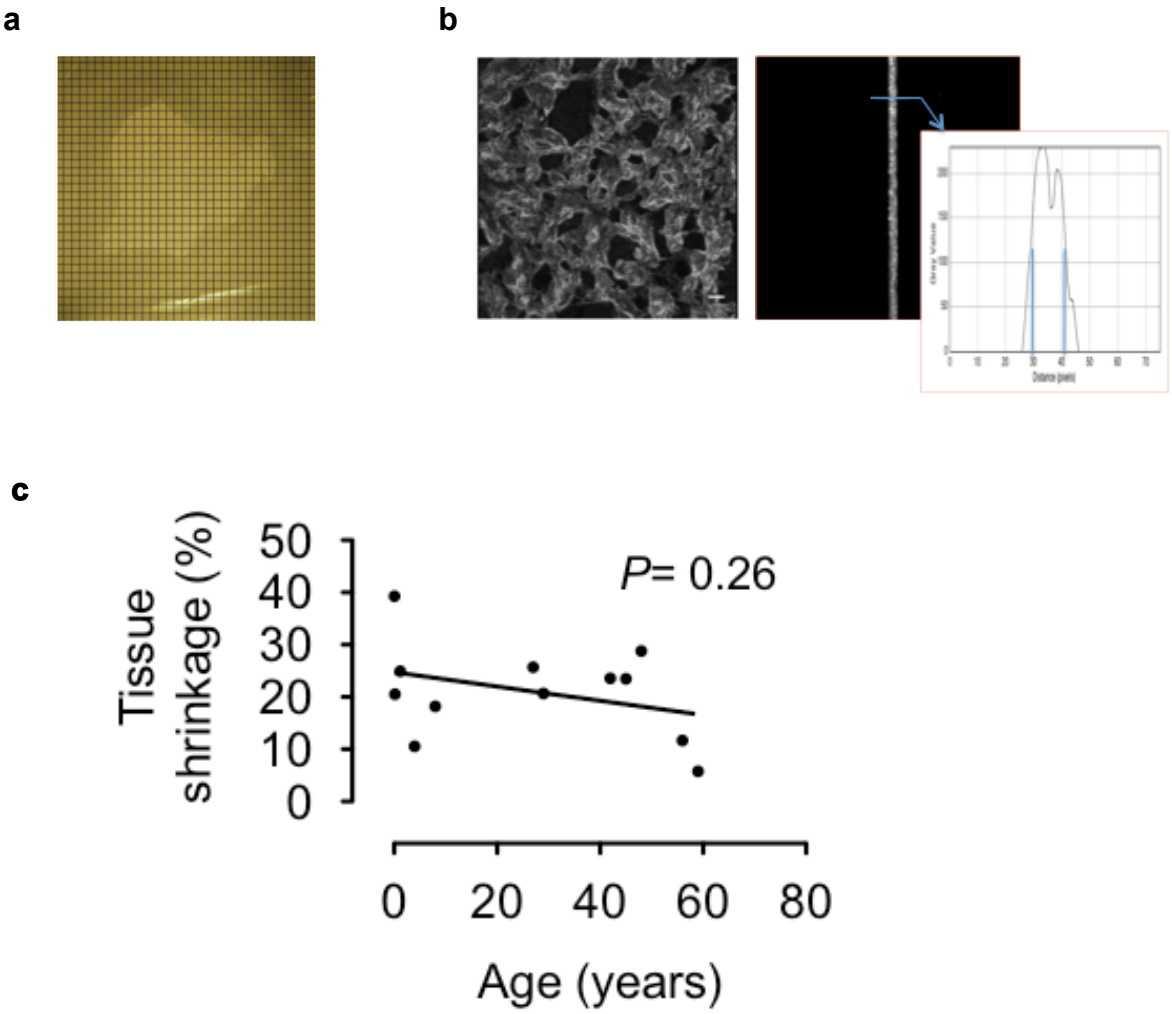

Supplemental Figure S6. Quantification of tissue shrinkage.

(**a**) A representative phase contrast image of an unfixed and unstained myocardial section from HS 5.114, overlaid with a grid with known dimensions for determination of the area shrinkage via grid-point method (xy-dimensions). (**b**) DIC images of Z-stacks of myocardial tissue sections with orthogonal view and grey value profile for determination of FWHM (full width at half maximum) intensity. (**c**) Volume shrinkage (%); linear regression analysis (P = 0.26) showed that the slope was not significantly different than 0. We calculated a mean value for tissue shrinkage of 21 % ± 5.8% (n = 12 hearts).

Supplemental Figure and Legend S7

a

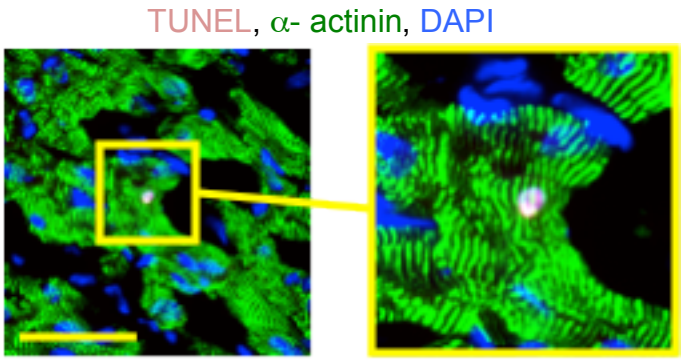

b

Sample ID	HS21-63	HS16-67	HS15-67	HS4-62	HS14-18
Age (years)	1.2	4	9	14	19
Total Area Quantified (mm^2)	73.15	69.14	135.12	120.05	86.65
TUNEL pos events	0	0	0	0	1

Supplemental Figure S7. Apoptosis is not a mechanism related to physiologic heart growth

To determine whether cardiomyocyte apoptosis is a mechanism associated with myocardial growth, two slides from 5 hearts were examined for the presence of TUNEL-positive cardiomyocytes. (**a**) Representative photomicrographfrom a 19-year-old individual. (**b**) Results of quantification show that TUNEL-positive cardiomyocytes are extremely rare.

Supplemental Figure and Legend S8

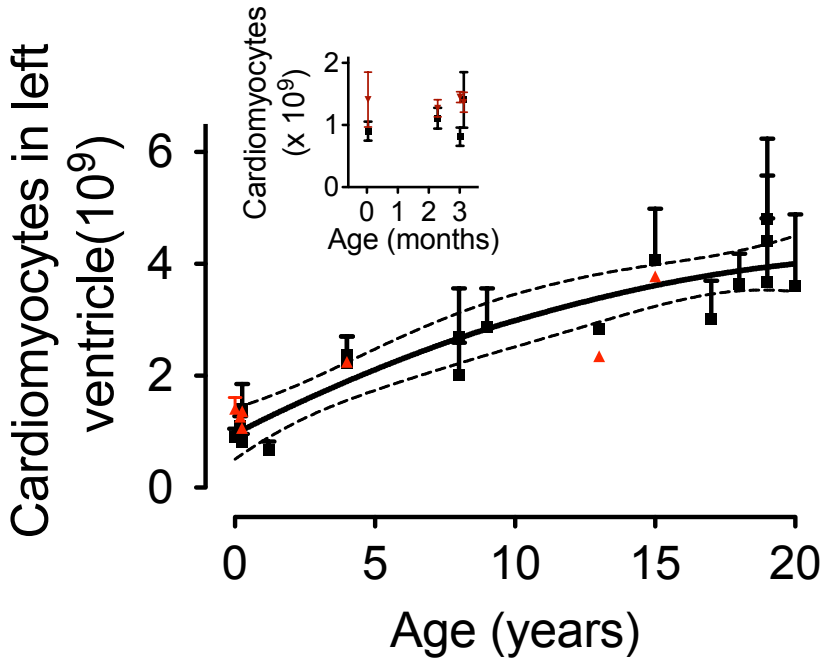

Supplemental Figure S8. Quantifications of cardiomyocyte number per LV using calculated and actual heart weights yield similar results.

Black dots indicate total number of cardiomyocytes per LV based on calculated heart weights from the donor's BSA. Red triangles indicate calculations based on the actual weights, which were available for 7 of the hearts. Blow-up graph of results in the first 3.5 months of life are shown.

Supplemental Table S1. List of all hearts used in this study.

#	Blinded ID	ID Number	Gen-der	Age	Histopathological comment	Cause of death
1.	HS60	M3873M	F	1 day	Focal haemmorhage of the atrioventricular valve. No other abnormalities	Stillbirth
2.	HS5	4.087	F	14 days	Normal myocardiym	Brain tumor, 11 days on life support
3.	HS61	1490	F	70 days	Unremarkable	Sudden unexpected death in infancy
4.	HS62	1738	F	92 days	Normal myocardium	Bronchopneumonia
5.	HS63	1055	M	96 days	Unremarkable	Bronchopneumonia
6.	HS21	5.114	F	1.2 y	Dense subendocardial fibrosis, slightly increased interstitial fibrosis	Drowning (hypoxic brain injury)
7.	HS4	4.043	M	3 y	Normal myocardium, no fibrosis or inflammation	Head trauma
8.	HS16	4.152	M	4 y	Normal myocardium	Motor vehicle accident-brain injury
9.	HS71	1185	M	4y	Unremarkable	Drowning
10.	HS28	5.144	F	4.5 y	No perivascular and/ or interstitial fibrosis, no inflammation	Hypoxic brain injury
11.	HS2	2.090	M	8 y	Normal myocardium	Not recorded
12.	HS31	3.109	M	8 y	Normal myocardium	Intracerebral hemorrhage
13.	HS15	5.110	M	9 y	Normal myocardium, only focal fibrosis within normal limits, no necrosis, no inflammation	Asphyxia
14.	HS72	5173	F	10y	No pathological change	Asthma
15.	HS73	1670	F	13y	Unremarkable	Asphyxia by hanging
16.	HS74	4638	M	15y	Unremarkable	Motor vehicle accident
17.	HS50	6.072	M	16 y	Markedly increased interstitial fibrosis	Hanged
18.	HS9	2.158	M	17 y	Normal myocardium	Head injury
19.	HS40	6.016	M	18 y	Slightly increased perivascular fibrosis, still within normal limits. No signs of other myocardial disease	Hypoxic brain injury-acute alcohol toxicity
20.	HS20	3.116	M	19 y	Normal myocardium	Motor vehicle accident
21.	HS27	3.168	F	19 y	Normal myocardium	Motor vehicle accident
22.	HS14	4.015	M	19 y	Plenty of regions with replacement fibrosis-abnormal	Hanging

#	Blinded ID	ID Number	Gen-der	Age	Histopathological comment	Cause of death
23.	HS23	1.103	F	20 y	Normal myocardium	Subarachnoid hemorrhage
24.	HS6	3.160	M	21 y		Motor vehicle accident
25.	HS1	5.138	M	23	Normal myocardium	Self-strangulation
26.	HS26	5.015	M	24	Normal myocardium	Not recorded
27.	HS19	5.048	F	25	Normal myocardium	SAB, not transplanted due to Herpes simplex serology
28.	HS29	3.135	M	26	Normal myocardium	Subarachnoidal haemmorhage
29.	HS7	2.116	F	27	Normal myocardium	Seizure
30.	HS13	5.054	M	27	Normal myocardium	Seizure
31.	HS32	5.086	M	29	Normal myocardium	Hypoxic brain injury
32.	HS3	5.003	M	37	Normal myocardium	Intracerebral haemmorhage
33.	HS34	3.069	F	40	Slightly increased focal, but no interstitial fibrosis. No necrosis. No inflammation.	Middle cerebral artery infarction
34.	HS12	5.041	F	42	Normal myocardium	Subarachnoidal haemorrhage
35.	HS18	1.095	F	45	Normal myocardium	Not recorded
36.	HS36	5.089	F	48	Normal myocardium	Subarachnoidal haemmorhage, no transplanted due to AB group incompatibility
37.	HS24	6.004	M	48	Markedly increased fibrosis	Hypoxic brain injury
38.	HS11	3.141	M	52	Normal myocardium	Intracerebral haemmorhage
39.	HS30	4.155	M	56	Normal myocardium	Hanging
40.	HS17	4.104	F	59	Normal	Not recorded

Legend to Supplemental Table S1. Myocardial tissue was provided by the NICHD Brain and Tissue Bank for Developmental Disorders at the University of Maryland and the University of Sydney. The samples were subjected to pathological evaluation and confirmed free of disease. Samples with increased fibrotic contents were taken out of the study (red).

Supplemental Table S2. Image acquisition hardware and settings.

	Hardware	Software and settings
Fig 1a-c	Olympus IX-81 epifluorescence microscope[3] with UPLFL ×10, and LUCPLFL ×40, NA 0.6 lenses and equipped with Hamamatsu EM CCD C9100	20–400 msec exposure, Slidebook[2]
Fig. 2 a,b	Olympus IX-81 epifluorescence microscope[3] with UPLFL ×10, and LUCPLFL ×40, NA 0.6 (immunofluorescence micrographs) lenses and equipped with Hamamatsu EM CCD C9100	20–400 msec exposure, Slidebook[2]
Fig. 3a	Olympus Fluoview 1000 epifluorescence microscope, 60x water objective, NA 1.2	100-600 msec exposure, Olympus software
Fig. 4c	Olympus IX-81 epifluorescence microscope[3] with UPLFL ×10, and LUCPLFL ×40, NA 0.6 (immunofluorescence micrographs) lenses and equipped with Hamamatsu EM CCD C9100	20–400 msec exposure, Slidebook[2]

Legend to Supplemental Table S2. Key to manufacturers: [1] Hewlett-Packard and Acuson; [2] Intelligent Imaging Innovations, Inc., Denver, CO; [3] CompuCyte, Westwood, MA

Supplemental Table S3. Quantification of numeric data.

Figure	Assay	Number of cardiomyocytes and/or hearts analyzed
Fig.1d	Fibrosis analysis	24 hearts analyzed, 20 sections per heart, 15 random images per section
Fig. 1e-f	Spot-to-spot variability of number of nuclei in different spots of the same LV	15 random systematic sections from 3 different, non adjacent parts of the LV
Fig. 2c	Mitotic cardiomyocytes (LSC)	651,160 cardiomyocytes
Fig. 3b	MKLP-1 positive events	15 images per sections analyzed, 20 sections per heart
Fig 4a	LSC validation of mononucleation assessment	1,500 cardiomyocytes manually counted from 5 different hearts
Fig. 4b	Mononucleated cardiomyocytes	220,989 cardiomyocytes
Fig. 4d	Cardiomyocyte ploidy validation by FISH	500 cardiomyocytes from 5 different hearts for each chromosome-specific probe (chromosomes X and 8)
Fig. 4e-f	Polyploid cardiomyocytes	Appr. 15 000 cardiomyocytes per sample counted
Fig. 5a	Cardiomyocyte nuclear density by optical dissector	3 random images of 5 sections (15 sample volumes per heart)
Fig. 5b	Cardiomyocyte nuclei	3 random images of 5 sections (15 sample volumes per heart)
Fig. 5c	Number of cardiomyocytes in LV	3 random images of 5 sections (15 sample volumes per heart)
Fig. 5d	Mean cardiomyocyte volume	1,928 cardiomyocytes

Supplemental Table S4. Antibody manufacturers and dilutions.

Antibody/dye	Manufacturer	Dilution/concentration
Phosphorylated histone H3 at Ser10 (H3P)	Millipore	1:500
MKLP-1	Abcam	1:100
Sarcomeric α-actinin (α-actinin)	Sigma	1:500
Tropomyosin CH1 (TM)	Developmental Studies Hybridoma Bank	1:100
Pan-cadherin (Cat #C3678)	Sigma	1:500
Caveolin 3 (Cat #610421)	BD Transduction Labs	1:100
Alexa- conjugated secondary antibodies	Invitrogen	1:200 to 1:500
DAPI	Invitrogen	50 nM
Cell mask orange	Invitrogen	5 μg/mL

Supplemental Table S5. Comparison of quantitative data of recent studies of cardiomyocyte generation and renewal in humans without evidence for heart disease.

		Bergmann et al., 2009	Kajstura et al., 2012, non-failing hearts			Mollova, Bersell et al., non-failing hearts		
Age	**Number of hearts/Results**	**Predicted CM generation (% per year)**	**Ki67 (%)**	**H3P (%)**	**Predicted CM generation (% per year)**	**H3P (%)**	**Cytokinesis (%)**	**Predicted CM generation (% per year)**
	Assay:	**^{14}C***	**Sections**	**Isolated CM**	**^{14}C***	**Isolated CM¶**	**Sections**	**H3P§**
0-1 years	Number of hearts studied	0	0	0	0	6	6	6
	Results	-	-	-	-	0.04%	0.015%	100%
1-10 years	Number of hearts studied	2 (1, 6 years)	3	3	3	4	4	4
	Results	NA	0.15%	0.01%	21%	0.02%	0.01%	4.5%
10-20 years	Number of hearts studied	1 (19 years old)	2	2	2	5	5	5
	Results	1.9%	0.05%	0.004%	9%	0.01%	0.005%	1.6%
21-40 years	Number of hearts studied	5	2	2	2	12	6	12
	Results	1%	0.04%	0.003%	6%	0.01%	Not detectable	0.7%
>40 years	Number of hearts studied	6	12	12	12	3	3	3
	Results	0.5%	0.07%	0.006%	5.6%	0.001%	Not detectable	0.04%

Legend: * Cardiomyocyte generation was calculated by birth-dating of cardiomyocytes based on the mean ^{14}C-concentration in nuclear DNA. ¶ H3P data were obtained with laser scanning cytometry (LSC). § Cardiomyocyte generation was calculated from the prevalence of H3P cardiomyocytes, corrected for multinucleation and polyploidization. Since above the age of 20 years, we did not detect cytokinesis, this suggests either of two possibilities: none of the H3P events resulted in cardiomyocyte division or our cytokinesis assay, although sensitive enough to detect 0.005% cardiomyocyte cytokinesis, is not sensitive enough to detect the low frequency of cardiomyocyte cytokinesis in adult hearts.

REFERENCES

1. Howard CV, Reed M (2005) Unbiased Stereology: Three-Dimensional Measurement In Microscopy. Oxford: BIOS Scientific Publishers.
2. Grierson AM, Mitchell P, Adams CL, Mowat AM, Brewer JM, et al. (2005) Direct quantitation of T cell signaling by laser scanning cytometry. J Immunol Methods 301: 140-153.
3. Haycock GB, Schwartz GJ, Wisotsky DH (1978) Geometric method for measuring body surface area: a height-weight formula validated in infants, children, and adults. J Pediatr 93: 62-66.
4. Muhlfeld C, Nyengaard JR, Mayhew TM (2010) A review of state-of-the-art stereology for better quantitative 3D morphology in cardiac research. Cardiovasc Pathol 19: 65-82.
5. Sluysmans T, Colan SD (2005) Theoretical and empirical derivation of cardiovascular allometric relationships in children. J Appl Physiol 99: 445-457.
6. Foster BJ, Mackie AS, Mitsnefes M, Ali H, Mamber S, et al. (2008) A novel method of expressing left ventricular mass relative to body size in children. Circulation 117: 2769-2775.